Available online at www.sciencedirect.com
SCIENCE DIRECT®
C. R. Chimie 8 (2005) 441–456
COMPTES RENDUS CHIMIE
http://france.elsevier.com/direct/CRAS2C/

Account / Revue

Liquid-phase alkylation of phenol with *t*-butanol over various catalysts derived from MWW-type precursors

Emil Dumitriu [a,*], Daniela Meloni [b], Roberto Monaci [b], Vincenzo Solinas [b]

[a] *Laboratory of Catalysis, Technical University of Iasi, 71 D. Mangeron Ave, 70050-Iasi, Romania*
[b] *Dipartimento di Scienze Chimiche, Università di Cagliari, Complesso Universitario Monserrato, s.s. 554 Bivio Sestu, 09042 Monserrato (CA), Italy*

Received 25 May 2004; accepted after revision 7 October 2004

Available online 12 February 2005

Abstract

Three types of MWW-based catalysts (MCM-22, MCM-36 and ITQ-2) were studied in the liquid-phase alkylation of phenol by *tert*-butanol (TBA). Ammonia adsorption calorimetry was applied to investigate the acid properties of zeolites with different framework topology and crystallinity. It was established that acid properties of MCM-22 family depend mainly of the solid Al-content (the Si/Al ratio varied from 9.1 to 46.0). Delamination of MCM-22 precursor (MCM-22(P)) leading to ITQ-2 results in the decrease of the total acidity and the increase of the intermediate acid sites concentration, while the pillaring process yielding MCM-36 affected mainly the total concentration of acid sites, the acid strength distribution being similar to the corresponding MCM-22 zeolite. The catalytic activity and selectivity of zeolite-based catalysts are discussed. The most active catalyst for the studied reaction was MCM-22 B (Si/Al ~ 15). The results obtained with MCM-22 as catalyst revealed that, despite the expectations due to the presence of 10-MR pores in the structure of this zeolite, no enhanced selectivity to *p-tert*-butyl phenol (*p*-TBP) is observed. This has been rationalized by the assumption that most of reactions occurring in this system take place on acid sites at or close to the external surface. This assumption is also supported by the similar catalytic selectivity of the MWW-derived structures (viz. MCM-36 and ITQ-2), which expose a higher concentration of external pockets. However, it is noticeable the high catalytic activity of MCM-22 zeolites for the liquid-phase alkylation of phenol by TBA that is comparable to the gas-phase activity of large pore zeolites like as HY or HM. ***To cite this article: E. Dumitriu et al., C. R. Chimie 8 (2005).***

Résumé

L'alkylation en phase liquide du phénol par le *t*-butanol en présence de divers catalyseurs dérivés de précurseurs du type MWW. Trois catalyseurs à base de précurseurs MWW (MCM-22, MCM-36 et ITQ-2) ont été étudiés dans la réaction d'alkylation du phénol par le *tert*-butanol (TBA) en phase liquide. La calorimétrie d'adsorption d'ammoniac a été utilisée pour examiner les propriétés acides de zeolites de différentes topologies et cristallinités. Il a été établi que les propriétés acides de la famille MCM-22 dépendent principalement de la teneur en aluminium (le rapport Si/Al a varié de 9,13 à 46,0). La délamination du précurseur MCM-22 à ITQ-2 a comme résultat une diminution de l'acidité totale et une augmentation de la concentration en

* Corresponding author.
E-mail address: edumitri@ch.tuiasi.ro (E. Dumitriu).

1631-0748/$ - see front matter © 2005 Académie des sciences. Published by Elsevier SAS. All rights reserved.
doi:10.1016/j.crci.2004.10.007

sites de force acide intermédiaire, alors que le procédé de pontage produisant MCM-36 a affecté principalement la concentration totale en sites acides, la distribution de la force acide étant similaire à celle de la zéolithe MCM-22 correspondante. L'activité et la sélectivité catalytiques des catalyseurs à base de zéolithes sont discutées. Le catalyseur le plus actif pour la réaction étudiée était l'échantillon MCM-22, avec Si/Al = 15. Les résultats obtenus avec MCM-22 comme catalyseur a révélé que, malgré les prévisions et en raison de la présence d'ouvertures à 10-tétraèdres dans la structure de cette zéolithe, la sélectivité dans le sens de la formation de *p-tert*-butyl phénol n'est pas augmentée. Ceci peut s'expliquer en supposant que la plupart des réactions survenant dans ce système se produisent sur les sites acides ou proches de la surface externe. La sélectivité catalytique similaire des structures MWW-dérivés (viz. MCM-36 et ITQ-2), qui expose un nombre plus élevé de poches externes, plaide aussi en faveur de cette hypothèse. Cependant, on remarque la haute activité catalytique des zéolithes MCM-22 dans l'alkylation de phénol par le TBA en phase liquide, qui est comparable à l'activité des zéolithes HY ou HM dans la phase gazeuse. ***Pour citer cet article : E. Dumitriu et al., C. R. Chimie 8 (2005).***

Keywords: MCM-22; MCM-36; ITQ-2; Phenol; *t*-Butanol; Alkylation

Mots clés : MCM-22 ; MCM-36 ; ITQ-2 ; Phénol ; *t*-Butanol ; Alkylation

1. Introduction

The *tert*-butylation of phenol is commercially carried out for the production of *p-tert*-butyl phenol (*p*-TBP) and di-*tert*-butyl phenols (DBP) that are industrially important compounds. *p*-TBP has wide spread application in the manufacture of varnish and lacquer resins, antioxidant for soaps, ingredient in de-emulsifiers for oil field, motor oil additives etc, while DBP are used in the production of substituted triaryl phosphates and antioxidant in food and other consumable items [1,2]. Butenes, methyl-*tert*-butyl-ether and *tert*-butanol (TBA) can be used as alkylating agents, and various acid catalysts, e.g., liquid acids, metal oxides, cation exchange resins, zeolites, etc. can be employed under appropriate conditions to get either C- or O-alkylated products.

Since homogeneous catalysts exhibit many problems with respect to their handling, safety, corrosion and waste disposal, various solid acid catalysts were evaluated to achieve good yields and selectivities to the desired alkylation products. Among them, the microporous crystalline aluminosilicates, i.e. zeolites, were distinguished because they combine high stability with excellent activity and selectivity. Thus, the *tert*-butylation of phenol (gas- or liquid-phase reactions) has been studied using different zeolite catalysts, like as: faujasite Y and dealuminated Y [3–6], beta [6–9], mordenite [6,10,11], ZSM-12 and MCM-22 [12].

Among other zeolites, MCM-22 is distinguished by an unusual structure. The framework topology of MCM-22 has been shown to consist of layers linked together along the *c*-axis by oxygen bridges and contains two independent pore systems [13,14]. Within the layers are two-dimensional sinusoidal 10-MR channels (4.1 × 5.1 Å), and between two adjacent layers are 12-MR supercages (~7.1 × 7.1 × 18.2 Å) communicating each other through 10-MR apertures (4.0 × 5.5 Å). In addition, its typical thin platelet morphology results in high external surface area.

This structure is formed from a layered precursor designated as MCM-22 precursor (MCM-22(P)) [15], which is able to condensate the silanol groups present on the layer surfaces by calcination, and leading to the formation of the 3D framework (MCM-22). The precursor can be also used as starting material to prepare the pillared structure known as MCM-36 [16] or the delaminated material known as ITQ-2 [17], Fig. 1.

As a matter of fact, MCM-22 zeolite shows three independent types of pores: sinusoidal channels, large supercages (with 10-MR opening) and large pockets (half of supercages) on the external surface (7.1 Å diameter and 7 Å depth, 12-MR opening) [14]. Therefore, acid catalyzed reactions can occur in the three locations, and their rate, selectivity and deactivation are largely dependent on the size and shape of pores and pore apertures.

Generally, it is admitted that the hemicage acid sites play a very important role in many catalytic reactions [18–22]. For instance, the acid sites of these pockets were shown to be responsible for the fast, selective, and stable alkylation of benzene with ethene and propene

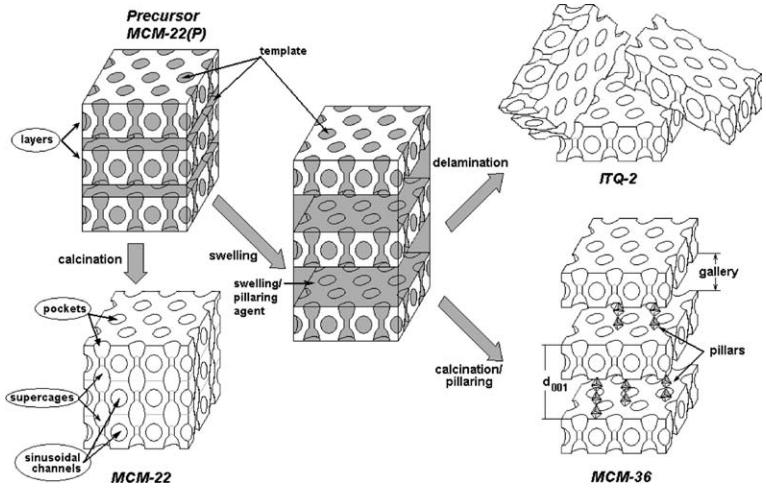

Fig. 1. Schematic illustration of the structure of MWW-based catalysts: MCM-22, ITQ-2 and MCM-36.

(e.g. [18]), and these properties are at the basis of commercial processes (e.g. Mobil/Badger-Raytheon EB-Max process for liquid-phase alkylation [23]). In order to prove the significant contributions of the pocket acid sites, various methods of investigation were applied, like as: test reactions, IR-spectroscopy, etc. For instance, choosing the *m*-xylene conversion as test-reaction, it was observed that in the large supercages with small apertures the isomerization into a 3.5 ÷ 1 *para–ortho* mixture is accompanied by *m*-xylene disproportionation; and most of the bulky trimethylbenzene products trapped in these cages undergo secondary transformations to smaller molecules or coke. At the same time, in the large external pockets, *m*-xylene is essentially transformed into a quasi-equimolar mixture of *para*- and *ortho*-xylenes, while in the narrow sinusoidal channels *m*-xylene transformation is practically limited to isomerization into the *para* product [24,25]. Moreover, by a selective deactivation of the acid sites of the supercages or of the external hemicages of a MCM-22 zeolite, it was evaluated the relative contributions of the protonic sites located in the supercages (ca. 42%), the external hemicages (22%) and the sinusoidal channels (36%) in *m*-xylene transformation. Additional proofs about the location of acid sites have been obtained by infrared spectrometry [26–29].

However, most of the other acid catalyzed reactions can occur on all the acid sites, as shown by selectivity values that are intermediate between those of large (12-MR, which allows bimolecular reactions involving bulky intermediates) and medium (10-MR, which gives rise to reactant and product shape selectivity) pore size zeolites [5–11].

The present work deals with the first study of the liquid-phase phenol alkylation by *t*-butanol over the three types of catalysts derived from MWW-type precursor: MCM-22, MCM-36 and ITQ-2. It was assumed that by pillaring and/or delamination the contribution of acid sites located on the hemicages will increase and it could be evidenced during the alkylation of phenol by *t*-butanol, process involving large reaction intermediates and products, which are difficult to be accommodated within sinusoidal channels. The MCM-22 zeolite was chosen as reference catalyst. Therefore, the catalytic activity and selectivity of these three types of materials are discussed and compared.

2. Experimental

2.1. Materials

The hydrothermal synthesis of the layered aluminosilicate MCM-22(P) was carried out by using hexamethyleneimine (HMI, 99%, Aldrich) as organic template, SiO_2 (Aerosil, Degussa), $NaAlO_2$ (56% Al_2O_3, 37% Na_2O, Carlo Erba), NaOH (98%, Prolabo) and deionized water. Based on the synthesis procedures previously reported [16,30,31], a typical sample with Si/Al = 15 (the most investigated sample in our study) was prepared as follows: sodium aluminate (0.68 g) and sodium hydroxide (1.18 g) were dissolved in 136.49 g

Table 1
Chemical composition and textural properties of MWW-based catalysts

Sample	Si/Al_{gel}	$Si/Al_{calcined}$	BET surface area S_{BET} (mg/g)	Micropore volume V_{micro} (cm^3/g)	Mesopore volume V_{meso} (cm^3/g)
MCM-22 A	8	9.1	499	0.179	0.07
MCM-22 B	15	14.7	583	0.207	0.06
MCM-22 C	20	20.6	586	0.213	0.10
MCM-22 D	30	29.8	429	0.154	0.06
MCM-22 E	50	46.0	357	0.128	0.05
ITQ-2	15	15.8	772	0.246	0.03
MCM-36	15	18.8	827	0.320	0.38

of deionized water. Then, 10.0 g of SiO_2 were added to this solution under stirring. After 30 min of stirring, the resulting gel was introduced into a Teflon-lined stainless-steel autoclave which was then rotated at 60 rpm, and heated at 150 °C for 220 h. After quenching the autoclave in cold water, the sample was filtered, washed thoroughly with deionized water until a pH lower than 9.0 was reached. Other samples with different Si/Al ratios (Table 1) were synthesized by the same procedure; only the time of crystallization was modified (e.g. the time of crystallization was increased for the samples with Si/Al ratio higher than 20).

MCM-36 was prepared according to the previously reported method [32]. The wet cake obtained as above (25–30% solids) was mixed with cetyltrimethylammonium chloride (CTMAC, 25%, Aldrich) and tetrapropylammonium hydroxide (TPAOH, Aldrich) with a relative weight ratio of 1:4:1.2 (MCM-22(P)/CTMAC/TPAOH). After the pH of the solution was adjusted to 13.5, the mixture was heated at 100 °C under continuous stirring for 68 h, then at room temperature for 4 h. The swollen material was recovered by filtration, then washed with a small amount of distilled water and dried at room temperature. Tetraethyl orthosilicate was added as pillaring agent to the swollen MCM-22(P) with a relative weight ratio of 5:1 (MCM-22(P)/TEOS). The mixture was heated at 90 °C for 25 h in a nitrogen atmosphere under continuous stirring. The solid material was recovered by filtration and dried overnight. Further, it was hydrolyzed in water with a 1:10 ratio (wt./wt., solid/water) under heating at 40 °C for 6 h during the hydrolysis, the pH of the mixture was adjusted at 1.9 with 1 M HNO_3 solution. Finally, the sample was calcined at 450 °C for 3 h in nitrogen and at 550 °C for 6 h in air (heating rate of 2°C/min).

ITQ-2 was synthesized by ultrasound delamination of a MCM-22(P) previously submitted to swelling by ion exchanging the initial HMI template agent by hexadecyltrimethylammonium as reported [33]. To swell MCM-22(P), we suspended 5.4 g of MCM-22(P) in 21.6 g of water, added 105 g of hexadecyltrimethylammonium bromide solution (29 wt.%) and 33 g of TPAOH (40 wt.%), the slurry pH was adjusted to 13.5 with an NaOH solution, and refluxed for 16 h at 80 °C. The layers in the swollen MCM-22(P) were stripped apart by placing the slurry in an ultrasound bath (50 W, 40 kHz) for 36 h at 25 °C. Finally, the solid phase was recovered by centrifugation (the pH of the slurry was slightly below 2). The collected material was calcined at 500 °C in order to remove the organic compounds.

The calcined zeolitic and related materials were ion-exchanged with an excess of 1 M NH_4NO_3 aqueous solution (liquid-to-solid ratio of 10 ml/g) and stirred continuously at 80 °C for 8 h. This procedure was repeated for three times. After being filtered and dried, the catalysts were calcined at 500 °C for 5 h (heating rate of 2 °C/min) in air to obtain protonated form.

2.2. Characterization

Powder XRD patterns were collected to estimate crystallinities and the structural changes of the synthesized materials on a SEIFERT diffractometer using Cu K_α radiation.

The chemical composition of the catalysts was measured by an inductively coupled plasma (ICP) method (LIBERTY 200, VARIAN spectrometer) after the digestion of the sample with HF solution.

The specific BET surface areas and the micropore volumes were determined by the nitrogen adsorption/desorption isotherms at –196 °C using a Micromeritics ASAP 2000 instrument. The samples were degassed at 300 °C and 10–3 Pa for 24 h prior to the adsorption

measurements. The specific surface areas were determined by the BET method. The micro- and mesopore size distributions were obtained from the adsorption branch of the isotherms. The pore volume and the average diameter of the pores were calculated by using t-plots.

The acid properties were evaluated by microcalorimetry. A Tian-Calvet flow equipment (Setaram) equipped with a volumetric vacuum line was used for microcalorimetric measurements. Each sample (100 mg) was pre-treated overnight at 400 °C under vacuum (10^{-3} Pa). Adsorption was carried out at 80 °C by admitting successive doses of ammonia and recording the thermal effect. The run was stopped at a final pressure of 133.3 Pa. Then, the sample was outgassed (10^{-3} Pa) for 1 h at the initial sorption temperature to eliminate the physisorbed ammonia

2.3. Catalytic reactions

The catalytic experiments were carried out in a small four-neck glass batch reactor (50 ml), equipped with magnetic stirrer, thermometer, and condenser. In order to avoid the lost of isobutylene formed during reaction the condenser was kept at –13 °C by the means of a cryostat. In a typical run, 10 mmol of phenol (PhOH), 6 mmol of TBA, 200 mg of freshly calcined catalyst, and 20 ml of solvent were used. The temperature was maintained at 70 °C (±0.5 °C) and the stirring rate was 800 rpm. Alkylation reaction was carried out at atmospheric pressure. Predetermined quantities of reactants and the catalyst were charged into the reactor and treated for 5 min into an ultrasounds bath in order to disperse the catalyst and to remove the adsorbed gases, and then the reactor was introduced into the thermostated bath at the desired temperature. The samples of the reaction mixture were withdrawn periodically and analyzed on HP 6890 Series on-line gas chromatograph equipped with a capillary column (Petrocol from Supelco, 50 m/l, 0.20 mm i.d., 0.50 μm film thickness). The temperature program was: 150 °C for 1 min, from 150 to 270 °C with a slope of 15 °C/min and at 270 °C during 10 min isothermally. The products of reaction were identified by means on GC-MS (HP 5890 Series for GC, HP5989A Series for MS) with FID detector and capillary column (Petrocol DH), carrier gas was Helium. Temperature program: from 150 °C with gradient 15 °C/min to 270 °C was used. Also, the products were identified by comparing them with genuine compounds.

3. Results and discussion

3.1. Characterization of catalysts

The composition and the main textural properties of catalysts obtained on the basis of MCM-22(P) are summarized in the Table 1. As it can be observed from this table, the Si/Al ratio of MCM-22 samples is approximately close to the gel composition. Generally, the amount of aluminium incorporated in the framework depends on the initial composition of the gel. There is a range of gel composition, the Si/Al ratio from 15 to 30, when the composition of zeolite is very close to the gel composition. Below or after this domain the composition of zeolite is more or less reach in aluminium than those of the gel. Comparing the different catalysts derived from the same MCM-22(P), it could be observed that the Si/Al ratio for ITQ-2 is different from those corresponding to the MCM-22 zeolite (MCM-22 B). This agrees with the assumption that during ultrasound treatment in basic medium dealumination or/and desilication processes occur [33]. As concerns the MCM-36 sample, it shows normally a higher Si/Al ratio due to the pillaring process (SiO_2 pillars). Also, it was reported that the swelling and pillaring processes could provoke a partial dealumination of the precursor [34].

All zeolitic materials (MCM-22 A...E) were found to be high crystalline phases on the basis of the x-ray diffraction. The transformation of the precursor to the MCM-22 zeolite resulted in an increase in the sharpness of the peaks. Also, it could be noted that the highest intensity was obtained on MCM-22 B (with Si/Al = 16.6).

Fig. 2 shows the XRD patterns of the catalysts derived from the same MCM-22(P). XRD and BET analysis (Table 1) revealed that ITQ sample is not completely delaminated (for instance, though the line characteristic of MCM-22 structure are scarcely visible due to the strong broadening, however, they yet exist), in agreement with the previous report [33]; in addition, a partial amorphization was observed. The XRD pattern of the MCM-36 sample is also presented in Fig. 2 and it could be remarked the apparition of a new peak (at 2θ between 1° and 2°) related to the pillared structure

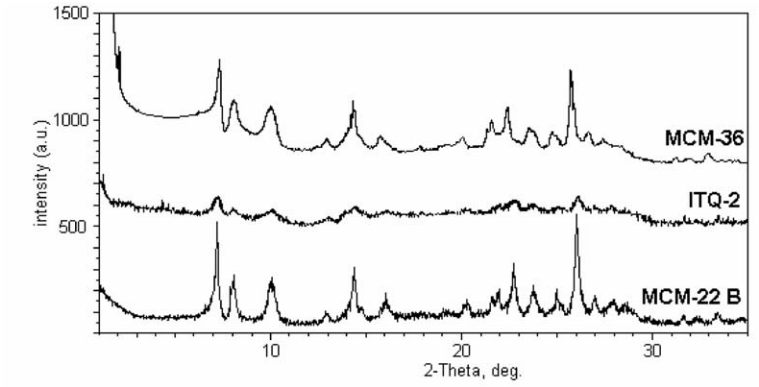

Fig. 2. XRD patterns of the catalysts synthesized from the same MCM-22(P).

(*d*-spacing). From the d_{001} value the distance between two layers of MCM-36 was calculated and it corresponds to approximately 24.9 Å, which agrees with the values reported before [13,32].

The BET surface area (S_{BET}), the micropore volume (V_{micro}) and the mesopore volume (V_{meso}) were evaluated from nitrogen adsorption/desorption isotherms and they are summarized in Table 1. For each type of catalyst the BET surface area and micropore volume agree well with the data of literature [33–35,38].

As concerns the MCM-22 zeolites, the surface area varies from sample A to E, and MCM-22 B (Si/Al = 14.7) and MCM-22 C (Si/Al = 20.6) show the highest surface areas. This variation could be correlated with sample crystallinity as far as the same variation was observed for the last property, the zeolite MCM-22 B showed the highest intensity in the XRD pattern. Also, a small fraction of mesopores was observed for MCM-22 catalysts (V_{meso} = 0.05–0.10 cm^3/g), and it is attributed to the agglomeration of the primary zeolite particles (thin platelets).

By delamination process the BET surface area of ITQ-2 increased for 1.7 times by comparison with the corresponding MCM-22 B sample obtained from the same precursor. Also, the pillaring process gave rise to the highest surface area corresponding to MCM-36 material (1.8 times higher than those of the MCM-22 B zeolite, but comparable with ITQ-2).

The acid properties of samples were estimated by adsorption microcalorimetry using ammonia as probe molecule. As known, this technique provides information about the number and the distribution of acid strength of the active sites. Calorimetric results are presented in Fig. 3, were the differential heats of adsorption are plotted versus ammonia uptake.

For each family of catalysts, the shape of the curves depends on the composition of the catalyst and its topology, and the plots are described more or less by stepwise curves. Generally, after the decrease of the differential heat with ammonia coverage, the microcalorimetric curves show a nearly horizontal plateau, which obviously is attributed to a homogeneous population of acid sites, and then they rapidly decrease at high ammonia coverage [36,37]. This pattern of behavior is especially pronounced for high Al-containing samples like as MCM-22 A and B. As the aluminium content decreases the plateau is considerably shortened (e.g. sample MCM-22 E), so that almost only a heterogeneous population of acid sites could be taken into account.

Therefore, as it can be seen from Fig. 3, the heats of adsorption continuously decrease with coverage for all samples and this shape is accounted for by the presence of the sites with different acid strength. The medallion from Fig. 3a illustrates the acidity spectra obtained by differentiating curve B and it shows more clearly the three regions of different acid strength: the strong and very strong sites (heats above 150 kJ/mol), the sites of medium strength (heats in the range of 150–100 kJ/mol), and the weak sites (heats between 100 and 70 kJ/mol, this latter value being often considered as a limit between chemisorption and physisorption in the case of ammonia).

The high differential heats for the most part of catalysts are in the range 211–260 kJ/mol at zero coverage, which indicates the existence of very strong sites (differential heats over 160–180 kJ/mol are predominantly associated with strong Lewis acid sites [36,37]); their concentration seems to be very low as indicated in Table 2.

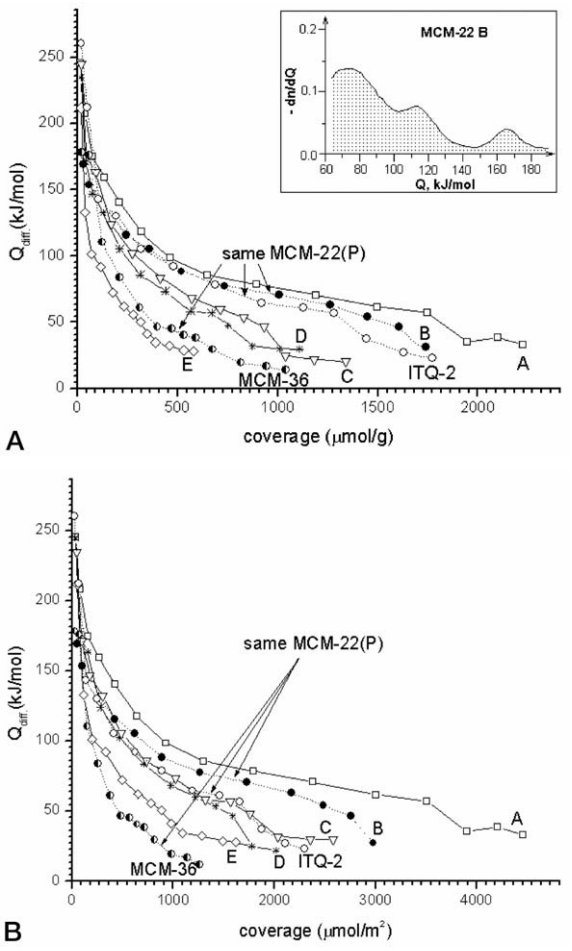

Fig. 3. Differential heats of adsorption of ammonia vs. coverage on MWW-derived catalysts; (a) ammonia coverage reported to the mass unit, (b) ammonia coverage reported to the surface unit; inset—the distribution of acid strength.

Only MCM-22 B and MCM-36 samples showed relatively small differential heats of 170–180 kJ/mol at zero coverage. Taking into account the heats of ammonia adsorption over 150 kJ/mol, the concentrations of strong acid sites decrease in the order:

B ≅ A > C > **ITQ-2** > **MCM-36** > D > E

Often, the total number of strong (Brönsted + Lewis) acid sites is represented by the V_{irr} value (the irreversible chemisorbed ammonia). This value is obtained by subtracting the adsorbed volume of the secondary isotherms from that of primary isotherms at the same equilibrium pressure (P = 0.2 Torr). According to the V_{irr} values, the concentration of strong acid sites is in the order:

A > B > **ITQ-2** > C > D > **MCM-36** > E

For MCM-22 family, results in Table 2 indicate that the concentration of the strong acid sites decreases with the solids Al-content. As known, the amount of strong acid sites is often close to the aluminium content of the zeolite, but higher aluminium content usually decreases the strength of these sites. This could be the explanation for the higher concentration of strong sites of the MCM-22 B sample (Si/Al = 14.7) than those of the corresponding MCM-22 A sample with the highest aluminium content (Si/Al = 9.13). Also, it is interesting to note that the V_{irr} values are better correlated with the total acidity:

A > B > **ITQ-2** > C > D > **MCM-36** > E

than with the concentration of strong acid sites (Q > 150 kJ/mol). We define the total number of acid sites (total acidity) of the catalyst as the amount of ammonia adsorbed with heats > 70 kJ/mol.

As concerns the sites of intermediate strength, obviously the heats of adsorption of 120(130)–160 kJ/mol

Table 2
Acid properties of MWW-based catalysts from microcalorimetric measurements

Sample	Si/Al	NH_3 ads. (μmol/g)				V_{irr} (P = 0.2 Torr) (μmol/g)
		70–120 kJ/mol	120–150 kJ/mol	>150 kJ/mol	Total >70 kJ/mol	
MCM-22 A	9.1	1000	158	212	1370	591
MCM-22 B	14.7	894	61	215	1170	562
MCM-22 C	20.6	394	84	153	631	247
MCM-22 D	29.8	325	120	86	531	227
MCM-22 E	46.0	153	21	48	222	57
ITQ-2	15.8	643	172	135	950	387
MCM-36	18.8	171	36	115	322	147

have been associated with Brönsted centers resulting mainly from bridging hydroxyls, whereas heats of adsorption in the range 100–120(130) kJ/mol represents weak Lewis sites. In this case, the concentration of intermediate strength sites (Q = 120–150 kJ/mol) decreases in the following order:

ITQ-2 > A > D > C > B > **MCM-36** > E

It could be observed that both the delaminating process and the pillaring process affect the acid properties of solids and such correlations cannot be established. Thus, ITQ-2 shows three times higher concentration of intermediate strength sites (173 μmol NH_3 per g) than MCM-22 B (61 μmol NH_3 per g), though both catalysts are obtained from the same MCM-22(P) (Si/Al_{gel} = 15).

Finally, it is worthy to note that the differential heat profiles for samples prepared from the same precursor (MCM-22(P)), viz. MCM-22 B, ITQ-2 and MCM-36, look quite different (Fig. 3). By comparing the three samples (Fig. 3) it is inferred that the effect of later treatment on the acid properties is very important. The simple calcination of MCM-22(P) lead to sample MCM-22 B, which shows microcalorimetric curves (Fig. 3a, b) characteristic to zeolitic materials. As for the delaminated sample, the shape of curve is comparable and close to that of the corresponding MCM-22 zeolite (Fig. 3a). With respect to the delamination process, though it could be supposed that by this process the concentration of acid sites per mass unit will increase due to the separation of zeolite layers; as a matter of fact, it decreases due to the partial amorphization, changes in the acid sites topology (by silicon or aluminium removal) and other effects (for example, the dislocation-induced defects). Apparently, the delamination reduces the density of acid sites due to the increase in specific surface area, thus the curve of differential heats from Fig. 3b is closer to MCM-22 C (with Si/Al ratio of 21), than that of the corresponding MCM-22 (sample B). Also, the delamination process changes the distribution of the acid strength. MCM-22 B has the ratio between the concentration of strong sites and the intermediate acid sites equal to 3.5, while for ITQ-2 this ratio is 0.78. For that reason, it could be assumed that the contribution of the sites of intermediate acid strength increases by delamination.

The pillaring process also results in strong decrease in the total acidity, but the acid strength distribution is lesser affected since the aforementioned ratio is of about 3.2, close to that corresponding to MCM-22 B. The decrease in acidity could be explained by the decrease of Al-content during the swelling and pillaring process [32].

3.2. Catalytic alkylation

As known, electrophilic alkylation of aromatics in the presence of an acid catalyst is commonly considered as proceeding via a carbenium ion type mechanism. Carbenium ion is formed during the dehydration of TBA or by protonation of resulted isobutene. Finally this ion is attacked by a free or weakly adsorbed aromatic hydrocarbon. to give O- and C-alkylated products as illustrated in Scheme 1. The subsequent alkylation leads to the di-substitued and tri-substituted phenols.

The MWW-based catalysts were tested in the *tert*-butylation reaction of phenol carried out at 343 K. In order to avoid the formation of large amounts of secondary products like as the oligomers of isobutene, the experiments were carried out by using a molar ratio of PhOH/TBA = 1:0.6. Generally, CCl_4 was used as solvent, the same as in our previous study concerning the alkylation of phenol over large pore zeolites [6]. The overall conversion of phenol and the evolution of the product selectivity versus the reaction time, for sample MCM-22 A, are illustrated in Fig. 4.

In our previous studies [6,11] concerning the phenol was alkylated with TBA in the presence of FAU-, BEA-, and MOR-type zeolites, it was noticed that O-alkylated product is formed in the earlier stages of reaction. The progress of this reaction depends on both the acid and the hydrophobic properties of the zeolite. The irreversible C-alkylation of phenol is the main reaction when the equilibrium of the O-alkylation reaction is shifted towards the hydrolysis of the aryl ether. Here, for MCM-22 sample, we observed a similar behavior for low conversion of phenol, when it is partially converted to *tert*-butyl-phenyl-ether (TBPE). However, after 4 h of reaction no trace of TBPE was found. As mentioned above, TBA cracks into isobutylene and water in the presence of acidic catalysts. Water thus formed in situ may have a detrimental effect on the catalyst activity resulting in low conversion of phenol, as well as on the catalytic selectivity. It was proved that on dried zeolite samples TBPE is formed in the initial

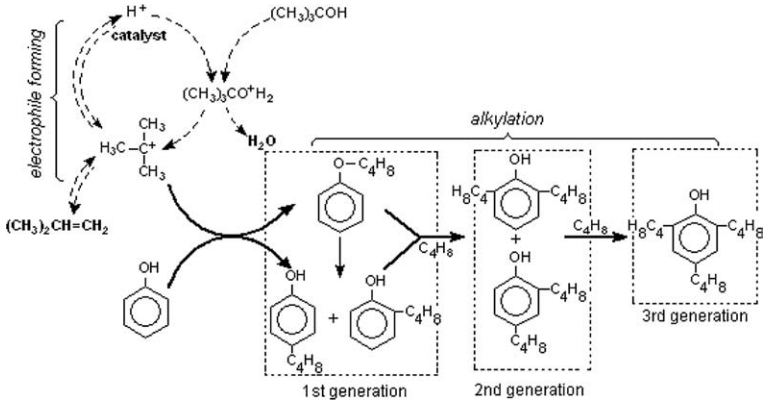

Scheme 1.

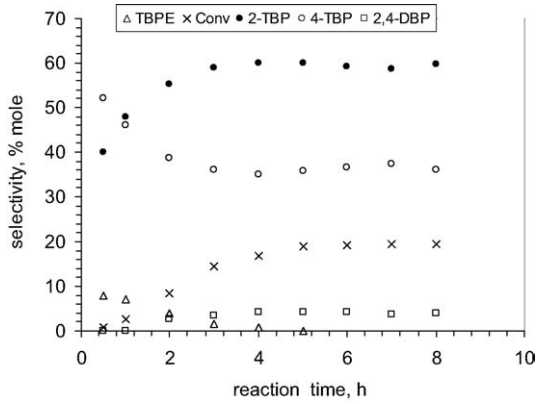

Fig. 4. Evolution of product selectivity over MCM-22 A (Si/Al = 9.1) catalyst; T = 70 °C, PhOH/TBA = 1.66 (mol/mol).

stage of reaction, while no amount of TBPE was observed on non-dried samples [6].

Also, it could be observed that the selectivity to the mono-alkylated product was very high and no oligomers formed. Subsequent experiments will confirm the high selectivity of MWW-based catalysts for mono-alkylation of phenol to the aromatic ring.

3.2.1. Effect of speed of agitation

The first steps to choose the proper conditions of reaction consisted in the investigation of the influence of agitation and quantity of catalyst on the catalytic performances in alkylation. The influence of external mass transfer on the reaction rate was studied by keeping the speed of agitation at 200, 600 and 900 rpm respectively. At high speed, 600–900 rpm, it was observed that the conversion of phenol was practically the same (Fig. 5) without any change in selectivity (Fig. 6). However, it is worthy to note that the lowest selectivity to

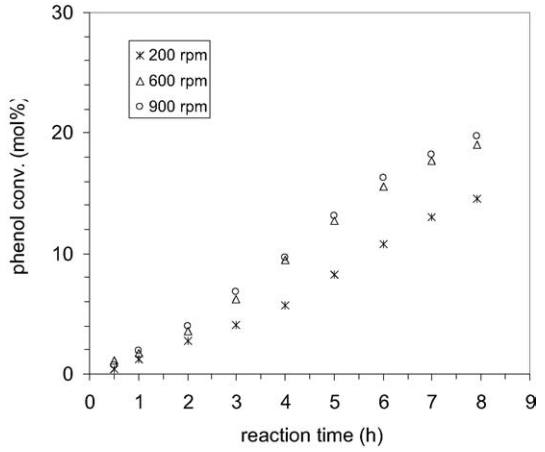

Fig. 5. Effect of speed of agitation on the phenol conversion by alkylation with TBA; P/TBA 1:0.6; temperature 70 °C, solvent CCl_4, catalyst MCM-22 B; catalyst loading 0.01 g/cm^3.

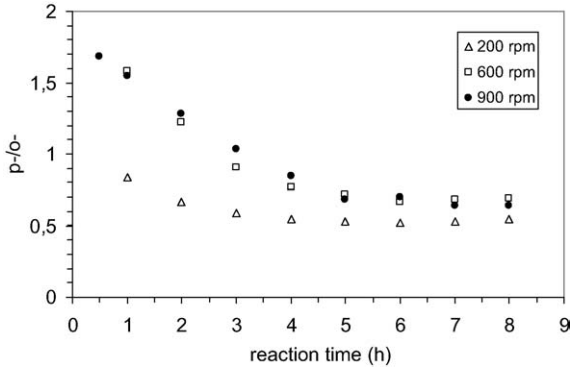

Fig. 6. Effect of speed of agitation on the selectivity to *t*-butyl phenols; P/TBA 1:0.6; temperature 70 °C, solvent CCl_4, catalyst MCM-22(15); catalyst loading 0.01 g/cm^3.

p-TBP is obtained at low speed of agitation. This behavior could be explained by taking into account the influence of the diffusion, which proceeds at low rate. Under these circumstances is likely that the isomerization of *p*-TBP to the *meta* isomer is favored because of long residence time in the pore system of MCM-22 zeolite.

Therefore, it might conclude that the alkylation of phenol by *t*-butanol was not influenced by external mass transfer effects when the speed of agitation is kept at high values. Hence, further experiments were carried out at 1000 rpm to be sure that there is no influence of the diffusion processes.

3.2.2. The influence of the amount of catalyst

In order to investigate the change in yield and selectivity of alkylated products, different amounts of catalysts were loaded in the batch reactor. With an increase in catalyst loading, the conversion of phenol also increased (Fig. 7) and this can be correlated with the increase in the number of active sites. At lowest catalyst loading, the conversion of phenol was only 14% and it increased to 46% when the loading was 0.01 g/cm^3. In the last case the conversion is comparable to that obtained for the gas-phase alkylation of phenol over large pore zeolites.

Fig. 8 illustrates the yields of mono-alkylated products vs. the reaction time for the three different amounts of catalyst. As it can be observed, when the loading of catalyst exceeds 0.005 g/cm^3 the amount of catalyst does not strongly influence the ratio between the two

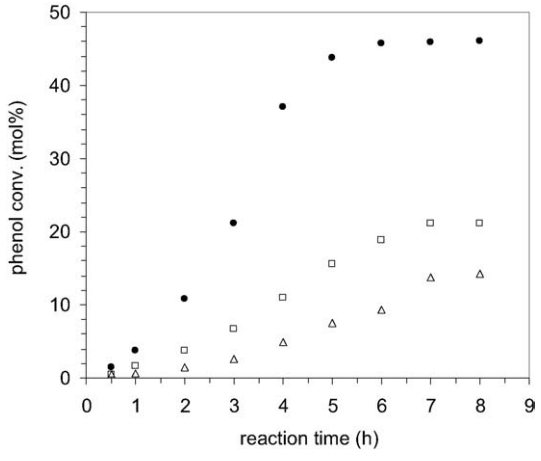

Fig. 7. Effect of catalyst loading on the phenol conversion with TBA; P/TBA 1:0.6; temperature 70 °C, speed 900 rpm, solvent CCl_4, catalyst MCM-22 B; (△) 0.00125 g/cm^3; (□) 0.005 g/cm^3; (•) 0.01 g/cm^3.

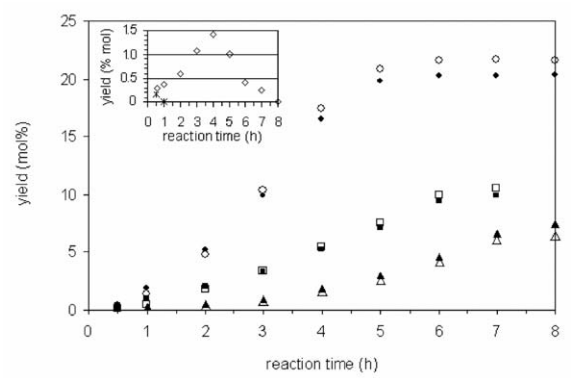

Fig. 8. Effect of catalyst loading on the distribution of mono-alkylated phenols; P/TBA 1:0.6; temperature 70 °C, speed 900 rpm, solvent CCl4, catalyst MCM-22(15); (open symbol) *para-t*-butyl-phenol; (black symbol) *ortho-t*-butyl-phenol; catalyst loading: (•, ○) 0.01 g/cm^3; (■, □) 0.005 g/cm^3; (▲, △) 0.00125 g/cm^3; medallion: (◇) TBPE at 0.0125 g/cm^3 catalyst loading, (✳) TBPE at 0.005 g/cm^3 catalyst loading.

isomers of *tert*-butyl-phenol. However, noticeable differences could be observed with regard to the formation of TBPE, though only very small amounts of ether were identified (see the medallion).

Interestingly, the amount of ether decreases as the loading of catalyst increases. Since the alkylation reactions were carried out at constant speed of agitation, constant temperature and fixed particle size, it may assume that the formation and the conversion of TBPE is intra-particle diffusion controlled. Also, a very small change in the distribution of mono-alkylated products could be observed for each catalyst loading, especially at longer reaction periods. As consequence, the further experiments were carried out using catalyst loading of 0.01 g/cm^3 that leads to higher conversions.

3.2.3. Effect of acid properties

In the literature, it is mentioned that the product distribution in the t-butylation of phenol over zeolite catalysts depends on the number of acid sites, their acid strength and the ratio of Brönsted to Lewis acid sites (e.g. [4]). On the other hand, it is well known that the acid properties of zeolites can be directly modified by synthesis (viz. Si/Al ratio, isomorphous substitution of aluminum) or by post-synthesis treatments (ion exchange, dealumination, chemical vapor deposition, etc.). For instance, incorporation of various trivalent cations into the framework, forming sites of metal osili-

cates, permits fine tuning of the acid strength of molecular sieves. At this stage, in order to obtain a correlation between the catalytic properties and acidity of the zeolite, it is interesting to study some of the factors affecting the zeolitic acidity, and their influence on the activity and product selectivity in phenol alkylation over zeolites. Hence, MCM-22 samples with different Si/Al ratios have been synthesized, as well as various ionic exchange processes were applied, then the resulting materials have been used as catalysts in the phenol alkylation by *t*-butanol.

3.2.3.1. MCM-22 with various Si/Al ratios. Fig. 9 shows the dependence of the conversion of phenol on the aluminium content (Si/Al ratio) of MCM-22 after different reaction times. It must be noted that similar behavior was observed for various reaction times. Variation of phenol conversion with Si/Al ratio could be correlated with the variation of the strong acidity, as measured by microcalorimetry ($Q > 150$ kJ/mol) and shown in Table 2. This correlation is better evidenced by the results obtained after 2 h of reaction. Afterwards, the water formed during the reaction probably influences the nature and the accessibility of acid sites.

The conversion of phenol in the alkylation reaction vs. the aluminum content of catalyst shows a maximum at Si/Al ratio approximately equal to 15, and then it decreases as the Al-content decreases. A similar behavior was observed for the Friedel-Crafts acylation of acetophenone by acetic anhydride in the presence of H-MCM-22 zeolites with different Si/Al ratios, as well as for the cracking of isooctane [37].

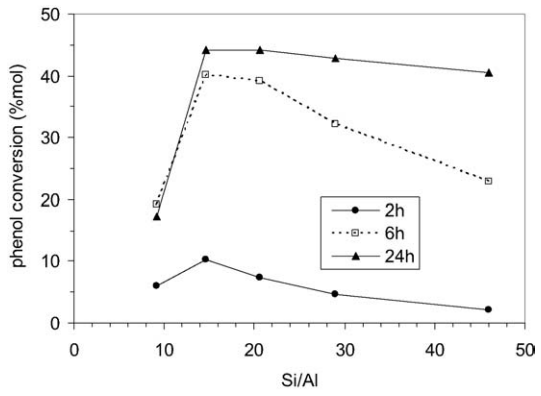

Fig. 9. Influence of the Si/Al ratio of MCM-22 zeolites on the phenol conversion; P/TBA 1:0.6; temperature 70 °C, speed 900 rpm, solvent CCl_4.

As concerns the selectivity to *p*-TBP, the influence of Si/Al ratio is very important for the first 2 h of reaction. During this period, as it can be seen from Fig. 10, the selectivity to *para* isomer shows a minimum that corresponds to the Si/Al ratio of ~15. For this zeolite composition, the microcalorimetric measurements showed the highest concentration (215 μmol NH_3 per g) of strong acid sites ($Q > 150$ kJ/mol, Table 2). As known, the strong acid sites favor the isomerization reactions. The selectivity to *para* isomer increases as the acid strength decreases.

3.2.3.2. The influence of the nature of compensating cations. Another method to tailor the acid–base properties of zeolites consists in the ionic exchange of the cations, which compensate the negative charges of zeolite framework. Fig. 11 illustrates the influence of the degree of Na^+ exchange on the initial rate of alkylation process. As it could be observed, the highest initial rate has been obtained at the lowest level of ion exchange by Na^+ cations. Then, the initial rate suddenly decreases and a linear correlation between the initial rate and the degree of ion exchange is obtained. It could be assumed that the most active protonic sites, perhaps on the external surface of crystals, are firstly exchanged by sodium cations and thus the initial rate of alkylation strongly decreases (see the line corresponding to the domain ranging between 10% and 20% degree of Na^+ exchange).

As concerns the influence of the degree of Na^+ exchange on the selectivity to the *para* isomer, only in earlier stage (i.e. the first 2 h of reaction, Fig. 12), it

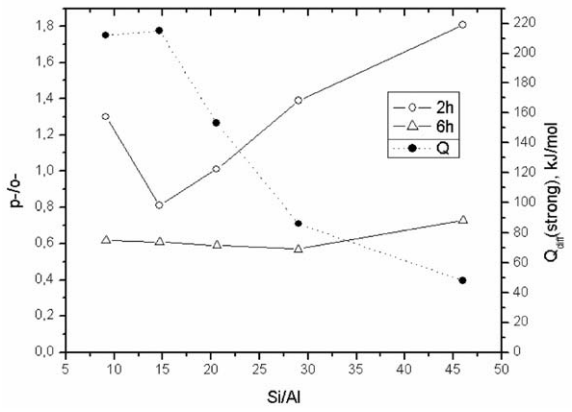

Fig. 10. Influence of the Si/Al ratio of MCM-22 zeolites on the selectivity to *p*-TBP; P/TBA 1:0.6; temperature 70 °C, speed 900 rpm, solvent CCl_4.

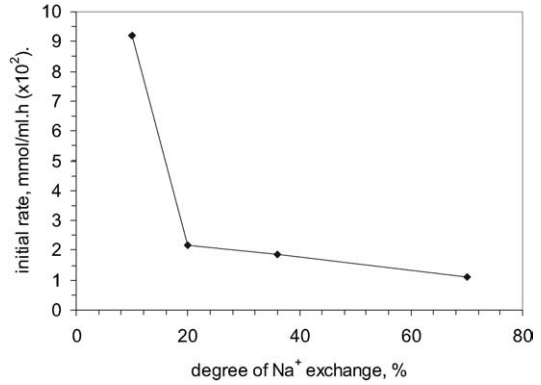

Fig. 11. Influence of the degree of Na^+ exchange on the conversion of phenol in *t*-butylation: catalyst MCM-22 B.

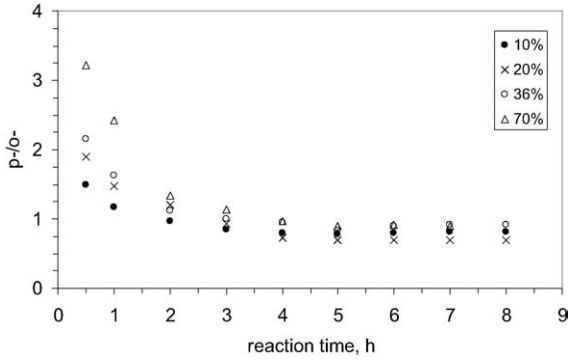

Fig. 12. Influence of the degree of exchange by Na^+ cations on the selectivity to *p*-TBP, catalyst MCM-22 B.

could be observed a significant influence, when three times more *p*-TBP is formed on the MCM-22 zeolite with the highest degree of exchange. That could be explained by the diminution of the concentration of the strong acid sites that reduces the rate of isomerization reaction. However, after 4 h of reaction the composition at equilibrium is reached.

In the second stage of alkylation, only 2,4-DBP is formed, and its amount depends on the degree of Na^+ exchange, Fig. 13.

3.2.4. The influence of the catalyst structure

In this work the performances of three types of catalysts based on the same MWW-precursor (the Si/Al ratio of gel was of 15) were examined for the alkylation of phenol with TBA, in the absence of mass transfer limitations (Figs. 14 and 15).

As it could be observed from Fig. 14, the shape of the kinetic curves is similar for all the catalysts indica-

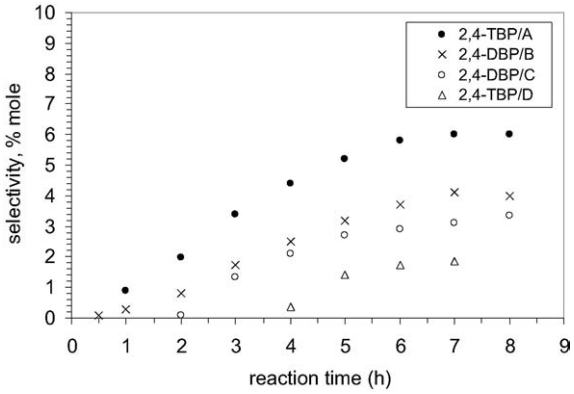

Fig. 13. Influence of the degree of exchange by Na^+ cations on the selectivity to 2,4-DBP, catalyst MCM-22 B.

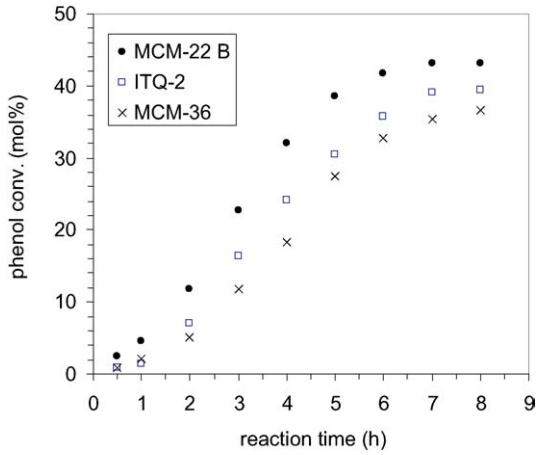

Fig. 14. Efficacies of various catalysts in alkylation of phenol with TBA; phenol/TBA 1:0.66, catalyst loading 200 mg, temperature 70 °C, solvent CCl_4.

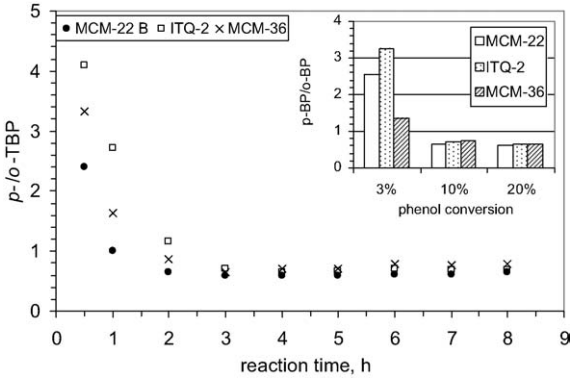

Fig. 15. Influence of catalyst structure on the selectivity to *p*-TBP; $T = 70$ °C, solvent CCl_4.

ting a similar catalytic behavior. However, contrary to our expectations, though both ITQ-2 and MCM-36 display more opened structures, and thus higher concentration of pockets on the external surface as compared with MCM-22, the highest activity is observed for the MCM-22 zeolite which, by contrary, has the most 'compact' structure. This behavior could be rather correlated with the acid properties of catalyst surfaces (Table 2). If we assume that the alkylation of phenol proceeds predominantly on the external surface, only those acid sites located on the external surface (mainly the pockets) contribute to the alkylation reaction. As the catalysts have been synthesized from the same precursor, it could be assumed that all the layers have the same Al-content (obviously, the acid properties of zeolites are associated to the presence of aluminum in the zeolite framework). For that reason, the two more open structures, ITQ-2 and MCM-36, should present the same catalytic activity or, at least, a similar activity, but higher than MCM-22. As the experimental data show all the other way, the explanation could be found in the delamination and pillaring process, which mainly affect the external acidity.

As concerns the influence of catalysts structure on the catalytic selectivity, it could be observed from the Fig. 15 that there are not spectacular differences and similar behavior is evidenced: for all the structures, the initial selectivity for the formation of *p*-TBP decreases with increasing reaction time.

Under the reaction conditions applied in the present study, the observed selectivities to alkylation products formed are close to those corresponding to the thermodynamic equilibrium. This observation probably indicates that diffusion or steric constrictions do not significantly influence the composition of *t*-butyl phenol isomers over these catalysts. In other words, the contribution of the acid sites inside sinusoidal channels to the alkylation reaction is significantly lower. The selectivity to *p*-TBP decreases when a more open zeolite structure is involved, like as the external pockets. These pockets are easily accessible for reactant molecules, and if a portion of the active sites is located in these pockets, the alkylation and particularly isomerization can proceed inside. The selectivity obtained with MCM-zeolite is quite comparable to that obtained with large pore zeolites [6].

Previous experiments in which di-*tert*-butyl-pyridine (DTBPy, 6.3 × 8.0 Å) was adsorbed on MCM-22 led to the conclusion that about 10% of acid sites are accessible for this bulky probe molecule [27]. It is without any doubt that the accessibility to the acid sites for the smaller phenol molecules should be higher than this percentage, and it could be also assumed that the acid sites close to the entrances of the 10-MR channels can be accessed by reagents during alkylation process. Therefore, 2,6-di-*tert*-butylpyridine was selected to passivate the external surface of MCM-22 without poisoning the internal acid sites according to Ref. [18], and the results of the alkylation reaction are presented in Fig. 16.

As shown in the medallion, a significant decrease in activity (half from the activity of the non-poisoned catalyst) resulted due to the partial neutralization of the external acid sites by the bulky DTBPy. Thus, it has to be concluded that the alkylation of phenol by TBA with MCM-22 takes place predominantly on the external surface. However, the plot of selectivity to various monoalkylated products vs. the conversion of phenol evidenced the existence of a small but constant *para*-selectivity. This selectivity should be explained only if the alkylation of phenol also occurs inside sinusoidal channels or, at least, to the entrance of 10-MR pores. Moreover, this experiment evidenced a possible sequence of reactions: firstly the O-alkylation takes place, and then the aromatic ring is alkylated in the *para* position. Further, as the reaction proceeds, *o*-TBP is formed either by direct alkylation or by the isomerization of *p*-TBP on the external surface. Thus, it seems that the contribution of the isomerization reaction is significant if we take into account the concave shape of curve

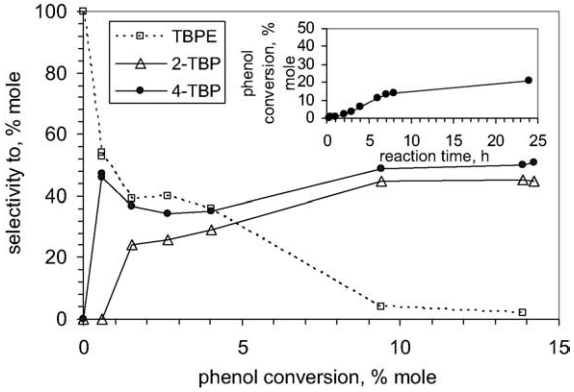

Fig. 16. Catalytic activity and selectivity of MCM-22 B partially poisoned by DTBP (~25% from the total acidity); reaction temperature 70 °C; solvent CCl_4.

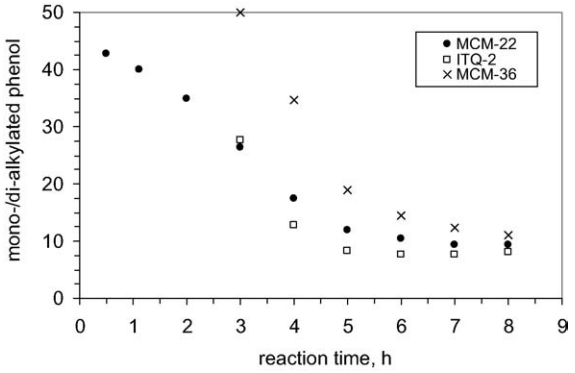

Fig. 17. Influence of catalyst structure on the selectivity to mono-alkylated phenol; 200 mg catalyst, P/TBA = 1.66; T = 70 °C, solvent CCl_4.

between 1% and 10% phenol conversion, which coincides with the increase in the selectivity to *o*-TBP.

The comparison among various catalysts derived from the same MCM-22(P) revealed another interesting feature. It was observed that both dialkylated products (2,4- and 2,6-di-*t*-butylphenol) are formed only in the presence of MCM-22 and ITQ-2 structures, while on the MCM-36 structures 2,4-di-*tert*-butylphenol is exclusively formed, Fig. 17.

We did not find an explanation for this behavior of the catalyst MCM-36. However, Fig. 17 shows that MCM-36 is the most selective catalyst towards mono-alkylated products.

3.2.5. The influence of solvent nature

Finally, we investigated the influence of various solvents on the alkylation process in the presence of MCM-22 B and MCM-36 catalysts. By comparison with CCl_4, the reaction rate increases when 1,3,5-triisopropylbenzene is used as solvent for both catalysts, and it decreases in the presence of *n*-octane or butyl acetate, Figs. 18 and 20.

Also, the selectivity to *para* isomer (it was defined as ratio between *para*- and *ortho*-TBP isomers) seems to be slightly influenced by the nature of solvent as data from Figs. 19 and 21 show.

The influence of solvent can be exerted either on the formation of charged intermediates, or by specific interactions with the reagents or products, or on the diffusivity of various species. The influence of solvent nature on the *tert*-butylation reaction was also observed for the alkylation of condensed polynuclear aromatic

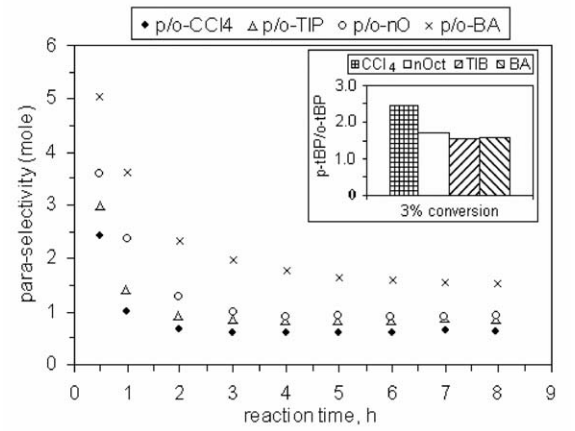

Fig. 19. Influence of the solvent nature on the *para*-selectivity, catalyst MCM-22 B, 200 mg, P/TBA = 1.66.

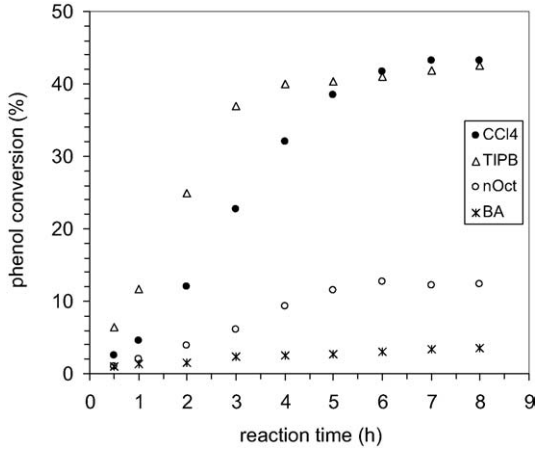

Fig. 18. Influence of the solvent nature on the conversion of phenol by alkylation, catalyst MCM-22 B, 200 mg, P/TBA = 1.66.

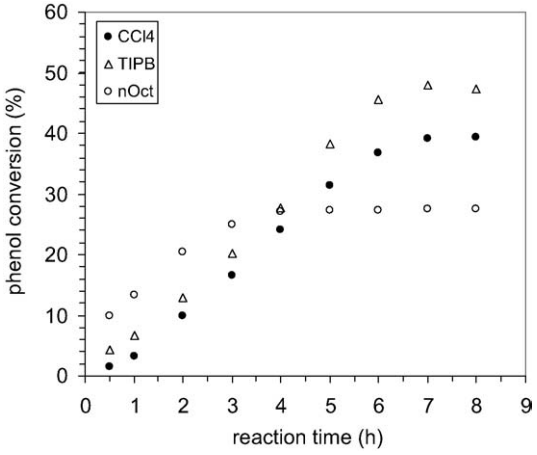

Fig. 20. Influence of the solvent nature on the conversion of phenol by alkylation, catalyst MCM-36, 200 mg, P/TBA = 1.66.

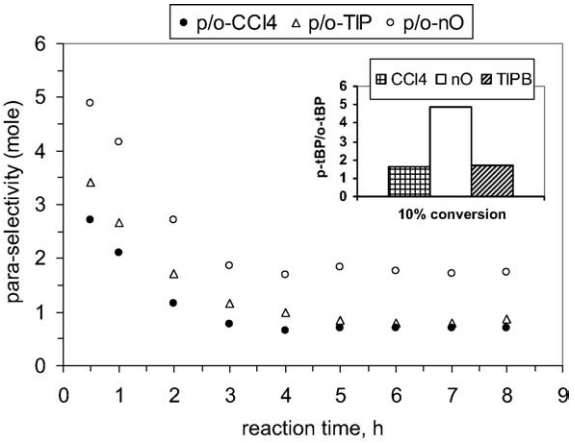

Fig. 21. Influence of the solvent nature on the *para*-selectivity, catalyst MCM-36, 200 mg, P/TBA = 1.66.

hydrocarbons [39]. By comparison with CCl_4, the authors found that the alkylation reaction in the presence of MCM-41, zeolite Y and the MOR- and BEA-type zeolites increases when isooctane was used as solvent.

4. Conclusions

Five MCM-22 samples with Si/Al ratios of 9–46 were hydrothermally synthesized together with two ITQ-2 and MCM-36 samples which were based on the same MCM-22(P) as sample MCM-22 B (Si/Al gel = 15). All the catalysts were characterized for their acid properties by ammonia adsorption microcalorimetry. The acid characteristics changed depending on the Al concentration and/or the method of synthesis. In the MCM-22 series the total acidity decreases with the Al-content decreasing, but the acid strength distribution revealed MCM-22 B (Si/Al ~ 14.7) as the strongest acid catalyst.

As concerns the ITQ-2 and MCM-36 samples, the method of syntheses affected the acid properties in a different manner. By comparing them with the corresponding MCM-22 structure, ITQ-2 showed approximately a close total acidity, but the concentration of the sites of intermediate acid strength is roughly three times higher. Contrariwise, the pillaring process strongly affected the total acidity of MCM-36 sample (approximately three times lower), but the acid strength distribution is similar to that corresponding to MCM-22 B sample. These features could be explained by the secondary processes of dealumination and/or desilication, which accompany the delamination and pillaring syntheses.

The alkylation of phenol with TBA in liquid-phase was investigated over acidic forms of the MWW-based catalysts, i.e. H-MCM-22, H-ITQ-2 and H-MCM-36. It has been found that the delamelation and pillaring did not improve the catalytic activity and this was explained by the secondary processes taking place during preparation of the corresponding materials, and thus affecting the acid properties. Also, it has been found that the *tert*-butylation reaction seems to preferentially proceed at or close to the external surface of the zeolite layers. Hence, the composition of the reaction products is not influenced to a considerable extent by product shape selectivity effects. As evidenced by experiments carried out on partially poisoned catalyst with DTBP, the main alkylation reaction consists in the electrophilic substitution of butyl radical in the *para* position, further followed by the rapid isomerization to *o*-TBP. After a longer period of reaction, the distribution of products approaches to the thermodynamic equilibrium. However, it is worthy to note that MCM-22 structures are efficient catalysts for the liquid-phase alkylation of phenol.

References

[1] J.S. Beck, W.O. Haag, in: G. Ertl, H. Knözinger, J. Weitkamp (Eds.), Handbook of Heterogeneous Catalysis, vol. 5, Wiley-VCH, Weinheim, 1997, p. 2131.
[2] A. Knop, L.A. Pilato, Phenolic Resins Chemistry, Springer, Berlin, 1985.
[3] A. Corma, H. Garcia, J. Primo, J. Chem. Res. 1 (1988) 40.
[4] R. Anand, R. Maheswari, K.U. Gore, B.B. Tope, J. Mol. Catal. A: Chem. 193 (2003) 251.
[5] K. Zhang, H. Zhang, G. Xu, S. Xiang, D. Xu, S. Liu, et al., Appl. Catal. A: Gen. 207 (2001) 183.
[6] E. Dumitriu, V. Hulea, J. Catal. 218 (2003) 249.
[7] K. Zhang, C. Huang, H. Zhang, S. Xiang, S. Liu, D. Xu, H. Li, Appl. Catal. A: Gen. 166 (1998) 89.
[8] P. Xu, B. Feng, S. Chen, Huadong Huagong Xueyuan Xuebao 14 (1988) 476.
[9] R.F. Parton, J.M. Jacobs, D.R. Huybrechts, P.A. Jacobs, Stud. Surf. Sci. Catal. 46 (1988) 163.
[10] K. Zhang, S. Xiang, H. Zhang, S. Liu, H. Li, React. Kinet. Catal. Lett. 77 (2002) 13.
[11] V. Hulea, E. Dumitriu, Prog. Catal. 10 (2001) 59.
[12] C.D. Chang, S.D. Hellring, US Patent 5 (1994) 288–927.
[13] M.E. Leonowicz, J.A. Lowton, S.L. Lawton, M.K. Rubin, Science 264 (1994) 1910.

[14] S.L. Lawton, M.E. Leonowicz, R.D. Partidge, P. Chu, M.K. Rubin, Micropor. Mesopor. Mater. 23 (1998) 109.
[15] M.K. Rubin, P. Chu, US Patent No. 4 954 325, 1990.
[16] C.T. Kresge, W.J. Roth, K.G. Simmons, J.C. Vartuli, US Patent 5 (1993) 229–341.
[17] A. Corma, V. Fornés, S. Pergher, T. Maesen, J.G. Buglass, Nature 396 (1998) 353.
[18] A. Corma, V. Martínez-Soria, E. Schnoeveld, J. Catal. 192 (2000) 163.
[19] R. Millini, G. Perego, W.O. Parker Jr., G. Bellussi, L. Carluccio, Micropor. Mater. 4 (1995) 221.
[20] P. Wu, T. Komatsu, T. Yashima, Micropor. Mesopor. Mater. 22 (1998) 343.
[21] S.-H. Park, H.-K. Rhee, Catal. Today 63 (2000) 267.
[22] J.S. Beck, A.B. Dandekar, T.F. Degnan, in: M. Guisnet, J.P. Gilson (Eds.), Zeolites for Cleaner Technologies, in: Catalytic Science Series, vol. 3, Imperial College Press, London, 2002, p. 223.
[23] J.D. Sherman, Proc. Natl Acad. Sci. USA 96 (1999) 3471.
[24] S. Laforge, D. Martin, J.-L. Paillaud, M. Guisnet, J. Catal. 220 (2003) 92.
[25] S. Laforge, D. Martin, M. Guisnet, Micropor. Mesopor. Mater. 67 (2004) 235.
[26] D. Meloni, S. Laforge, D. Martin, M. Guisnet, E. Rombi, V. Solinas, Appl. Catal. A: Gen. 215 (2001) 55.
[27] A. Corma, V. Fornés, L. Forni, F. Marquez, J. Martinez-Triguero, D. Moscotti, J. Catal. 179 (1998) 451.
[28] A. Corma, U. Diaz, V. Fornés, J.M. Guil, J. Martinez-Triguero, E.J. Creyghton, J. Catal. 191 (2000) 218.
[29] B. Onida, L. Borello, B. Monelli, F. Geobaldo, E. Garrone, J. Catal. 214 (2003) 191.
[30] A. Corma, C. Corell, J. Pérez Pariente, Zeolites 15 (1995) 2.
[31] A. Corma, V. Fornés, J. Martínez-Triguero, S.B. Pergher, J. Catal. 186 (1999) 57.
[32] Y.J. He, G.S. Nivarthy, F. Eder, K. Seshan, J.A. Lercher, Micropor. Mesopor. Mater. 25 (1998) 207.
[33] R. Schenkel, J.-O. Barth, J. Kornatowski, J.A. Lercher, Stud. Surf. Sci. Catal. 142 (2002) 69.
[34] J.-O. Barth, R. Schenkel, J. Kornatowski, J.A. Lercher, Stud. Surf. Sci. Catal. 135 (2001) 136.
[35] I. Rodriguez, M.J. Climent, S. Iborra, V. Fornes, A. Corma, J. Catal. 192 (2000) 441.
[36] A. Auroux, Top. Catal. 4 (1997) 71.
[37] A. Auroux, Top. Catal. 19 (2002) 205.
[38] K. Okamura, M. Hashimoto, T. Mimura, M. Niwa, J. Catal. 206 (2002) 23.
[39] E. Armengol, A. Corma, H. Garcia, J. Primo, Appl. Catal. A: Gen. 149 (1997) 411.